

Worst case SAR scenario as a new metric for SAR analysis in B1 phase shim

X. Wu¹, T-H. Chang², Z-Q. Luo², C. Akgun¹, J. Vaughan¹, K. Ugurbil^{1,3}, and P-F. Van de Moortele¹

¹Center for Magnetic Resonance Research, University of Minnesota, Minneapolis, MN, United States, ²Department of Electrical and Computer Engineering, University of Minnesota, Minneapolis, MN, United States, ³Max Planck Institute for Biological Cybernetics, Tübingen, Germany

Introduction: It has been shown numerically and experimentally that B_1 shim can efficiently address transmit B_1 (B_1^+) inhomogeneity (1). However, the risk of increasing specific absorption rate (SAR) deposition with RF manipulation is a major concern especially at very high magnetic field. The impact of B_1 shim on SAR has been considered but it remains difficult to compare SAR maps obtained with multi-transmit RF coils with a variety of phase and amplitude inputs. Here we propose a new metric, "pixel-wise worst case SAR scenario", to be used as a reference when comparing SAR for different B_1 shim solutions. Computing this reference, based on electromagnetic models, consists of finding the maximum $|E|^2$ ($|E|_{\max}^2$) value for each pixel for all of possible B_1 input complex values. We propose a fast computational solution for solving this nonconvex optimization problem, and we apply this method to generate $|E|_{\max}^2$ maps for 16-channel RF coils at 7 T.

Theory: For simplicity, we consider here the worst case SAR for " B_1 phase shim" where only B_1 phase of individual channels is adjusted while using a uniform RF magnitude through all channels. For N -channel transmission, the electric field (E field) is determined by $E = E_p$ where $E \in \mathbb{C}^{3 \times N}$ involves the E field maps and $p \in \mathbb{C}^N$ contains N RF inputs. Now we seek to maximize SAR at a location by adjusting the input RF phase on each channel. Since $\text{SAR} \propto |E|^2$, maximizing SAR at a location is equivalent to maximizing $|E|^2$. Then the corresponding optimization problem is $\max (E_p)^H E_p$ subject to (s.t.) $|p_n| = 1, n = 1, \dots, N$ [1], where $p \in \mathbb{C}^N$ is the optimization variable and the superscript H denotes complex conjugate transpose. Considering the fact that $(E_p)^H E_p = \text{trace}(p^H E^H E p) = \text{trace}(E^H E p p^H)$ and introducing $P = p p^H$ (which means $P \succeq 0$ and $\text{rank}(P) = 1$), we can rewrite problem [1] as its equivalent: $\max \text{trace}(E^H E P)$ s.t. $[P]_{n,n} = 1, n = 1, \dots, N, P \succeq 0, \text{rank}(P) = 1$ [2], where $P \in \mathbb{C}^{N \times N}$ is the variable and $[P]_{n,n}$ denotes the n -th diagonal element of matrix P . Now it's evident that problem [2] is nonconvex (because of the rank-1 constraint) and hence very hard to be solved. Fortunately, this problem can be accurately approximated using the semidefinite relaxation (SDR) technique (2) according to recent advances in optimization theory. This relaxation technique consists of two steps. The first step is to solve a rank relaxed version of problem [2] $\max \text{trace}(E^H E P)$ s.t. $[P]_{n,n} = 1, n = 1, \dots, N, P \succeq 0$ [3]. Note that problem [3] does not have the rank-1 constraint and thus is a convex optimization problem which can be very efficiently solved (3). The second step is to find an approximate solution using a simple randomization procedure based on P^* which is the optimal solution of problem [3]. In this randomization step, we first generate M vectors, $q^{(m)} \in \mathbb{C}^N, m = 1, \dots, M$, from the complex normal distribution $\mathcal{N}(0, P^*)$ and then determine $p^{(m)}$ by individually normalizing each component of $q^{(m)}$, i.e., $p_n^{(m)} = q_n^{(m)} / |q_n^{(m)}|$. The $p^{(m)}$, which gives the maximum value of $|E|^2$, is chosen as the approximate solution of problem [1]. It has been theoretically proven (2) that the worst case ratio of the objective value evaluated by the approximate solution to the optimal objective value of problem [1] is greater than $\pi/4$ (0.7854), which justifies at least 78% accuracy of this approximation method. With our specifications of B_1 phase shim, we found that this ratio was typically greater than 0.98 for $M = 100$.

Methods: In this study we considered two 16-channel RF stripline coil arrays. One is a large circular coil of 32 cm in diameter (4), and the other a small elliptical coil with 24 cm in major axis and 20 cm in minor axis (5). These two coils were modeled in XFDTD (Remcom Inc.), and their electromagnetic field maps were simulated when loaded with a human head. For each coil, we obtained the $|E|_{\max}^2$ map within an axial slice of the head by finding the SDR approximate solution of problem [1], one pixel at a time. The relaxed problem [3] was solved using SDPT3 (6). The number of random vectors, M , was set to 100 in the randomization step. We studied the effect of coil size on the $|E|_{\max}^2$ map by comparing the $|E|_{\max}^2$ map with its corresponding $|E|_{\text{SOM}}^2$ map determined by the sum of E field magnitudes (SOM), $|E|_{\text{SOM}}^2 = (\sum_{n=1}^N |E_{x,n}|)^2 + (\sum_{n=1}^N |E_{y,n}|)^2 + (\sum_{n=1}^N |E_{z,n}|)^2$. In order to further illustrate the readability of SAR maps normalized to the proposed $|E|_{\max}^2$ reference, we also compared SAR for two different sets of B_1^+ phases. In one setup the same input RF phase was used for all channels (equal phase). In the other setup the phases were determined azimuthally based on the coil geometry (geometric phase) with a phase increment of 22.5° per channel. The $|E|^2$ map was computed for each case, and the two $|E|^2$ maps were compared based on the ratio, $|E|^2 / |E|_{\max}^2$. All computations were performed in Matlab (MathWork Inc.).

Results: The $|E|_{\max}^2$ maps of the two coils exhibited similar patterns of $|E|_{\text{SOM}}^2$ map with $|E|^2$ values higher in the periphery than in the center, but the $|E|_{\max}^2$ map of the small elliptical coil was closer to the $|E|_{\text{SOM}}^2$ map than that of the large coil in terms of the ratio $|E|_{\max}^2 / |E|_{\text{SOM}}^2$ (Fig. 1). For most pixels with both coils the ratio $|E|_{\max}^2 / |E|_{\text{SOM}}^2$ was greater than 0.5. Interestingly, the small coil generated more pixels with a ratio greater than 0.8 than the large coil (92 vs. 69%, Fig. 2) suggesting a lower level of destructive interferences between complex E field vectors. As shown in Fig. 3, the geometric phase setup resulted in higher $|B_1^+|$ and lower $|E|^2$ in the central area than the equal phase setup (Fig. 3a,b,d and e). The ratio values with equal phase were close to the maximum of 1 in the center, while those of geometric phase were much lower (Fig. 3e and f), suggesting that, in the center, complex B_1^+ and E field interferences tend to have opposite trend (when constructive for one, destructive for the other and vice versa). With equal phase, the ratio distribution was clearly shifted to the right (Fig. 4) compared with the geometric phase setup.

Discussion and Conclusion: We introduce utilizing $|E|_{\max}^2$ maps, which determine a worst case SAR for each pixel, as a metric for SAR analysis with multi-transmit coils. We demonstrate an effective method to find the maximum $|E|^2$ for all B_1 phase shim combinations, based on an optimization problem approximated with the semidefinite relaxation technique. We also demonstrate, using 16-channel RF stripline arrays at 7 T, that such $|E|_{\max}^2$ map can help characterizing SAR patterns for different coils and different B_1 shim setups. (Actual SAR values require multiplying $|E|^2$ field by tissue conductivity/density which is omitted here for simplicity.) In the implementation described above only B_1 phases were modulated to determine $|E|_{\max}^2$, which could be seen a serious limitation. We can actually use an optimization criterion similar to problem [1], but with inequality constraints (i.e., $|p_n| \leq 1$ instead of $|p_n| = 1$) in order to find maximum $|E|^2$ values for B_1 shim, in which case both magnitude and phase of input RF are manipulated. This new optimization problem can also be approximately solved with SDR (7), but is computationally more demanding than problem [1]. However, we found that $|E|_{\max}^2$ maps obtained for B_1 phase and magnitude shim are very close to that for B_1 phase shim only, indicating that the $|E|_{\max}^2$ map for B_1 phase shim can be obtained and used for SAR analysis in B_1 phase and magnitude shim. Thus, it would be more time efficient to utilize the highest input magnitude utilized in a given B_1 shim set to quickly generate worst case scenario maps based on the faster, B_1 phase shim based method.

References: 1. G. Metzger, *et al.*, MRM in press. 2. S. Zhang, *et al.*, SIAM J. OPTIM 2006, 16(3):871-890. 3. S. Boyd *et al.*, *Convex Optimization*, Cambridge, 2004. 4. C. J. Snyder, *et al.*, ISMRM 2006, p.421. 5. G. Adriany, *et al.*, ISMRM 2005, p.673. 6. K. Toh, *et al.*, SDPT3 4.0 (beta), 2006. 7. Z. Luo, *et al.*, SIAM J. OPTIM. 2007, 18(1):1-28. **Acknowledgments:** This work was supported by BTRR - P41 RR008079, KECK Foundation, R01 MH070800 and U.S. NSF Grant DMS-0610037.

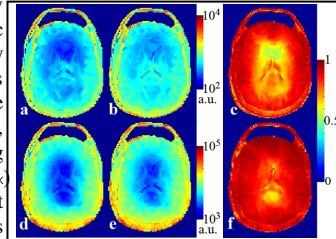


Fig. 1. Comparison of large (top row) and small (bottom row) coil. a,d: $|E|_{\max}^2$ maps. b,e: $|E|_{\text{SOM}}^2$ maps. c,f: ratio maps of $|E|_{\max}^2 / |E|_{\text{SOM}}^2$.

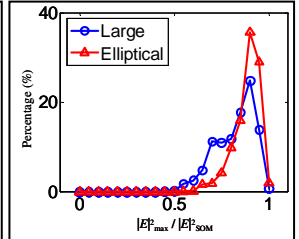


Fig. 2. Comparison of a large and a small elliptical coil in terms of percentage vs. ratio maps of $|E|_{\max}^2 / |E|_{\text{SOM}}^2$.

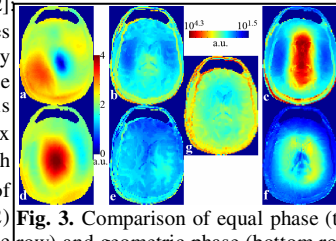


Fig. 3. Comparison of equal phase (top row) and geometric phase (bottom row) setups in B_1 phase shim using a large coil. a,d: $|B_1^+|^2$ maps. b,e: $|E|^2$ maps. c,f: ratio maps of $|E|^2 / |E|_{\max}^2$.

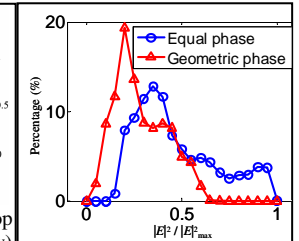


Fig. 4. Comparison of equal phase and geometric phase setups.